

OBSERVATIONS ON THE USE OF A TRACK-SENSITIVE TARGET  
IN THE 15-FOOT BUBBLE CHAMBER

P. Ermolov  
Serpukhov Institute of High Energy Physics

and

F. A. Nezrick  
National Accelerator Laboratory

ABSTRACT

The utility of a track-sensitive target in neutrino experiments is discussed in view of the following aspects:

1. photon-conversion efficiency
2. cost of chamber filling
3. neutrino flux through the target
4. background events outside the target
5. setting error when using a target
6. optical distortions of a track-sensitive target.

INTRODUCTION

The advantages and utilization of a track-sensitive target (TST) in a cryogenic bubble chamber have been profusely reported in previous summer-study reports.<sup>1-8</sup> We will not duplicate the previous works but intend to comment on the more general aspects of the TST technique. The parameters of the bubble chamber and TST used herein are given in Table I.

The principal advantages of a TST configuration compared to a pure chamber filling are (1) that one can analyze interactions with "free" protons and neutrons (inside the TST) by using a higher Z liquid around the target region, thereby obtaining a higher photon-conversion efficiency, (2) that it becomes economically desirable to separate the production region (TST) and the analysis region of the bubble chamber since the filling of the production region is in general more expensive than that for the analysis region.

The principal disadvantages of a TST configuration are that (3) the TST intercepts only a fraction of the flux passing through the bubble chamber yielding lower usable event rates inside the TST, (4) the ratio of events outside the TST to inside the TST is

large and introduces an unwanted background, (5) the setting error will be a function of position in the bubble chamber depending on whether or not the track is viewed through the TST, and (6) the apparent positions and directions of the tracks become distorted when viewed through the TST.

#### A. Photon-Conversion Efficiency

If the chamber is not fitted with a TST, then photons from  $\pi^0$ 's produced in primary-beam interactions will have an average potential length (i. e., length along the photon-flight path from the interaction point to the edge of the chamber) of about 2.5 m. If the chamber is filled with hydrogen ( $X_0 = 9.7$  m), then the probabilities of a single photon and 2 photons from a  $\pi^0$  converting in the chamber are 18% and 3.2% respectively.

To make constrained fits to  $1\pi^0$  or possibly  $2\pi^0$  events and still maintain the interactions on "free" nucleons, it is necessary to surround the target region with a track-sensitive liquid of shorter radiation length. The use of track-sensitive neon and neon-hydrogen mixture surrounding a track-sensitive hydrogen target have been tested<sup>9</sup> and have been found to work satisfactorily. Using the chamber dimensions given in Table I, the average potential length outside the TST in the forward direction is about 80 cm. If 15 cm is needed to identify and measure the converted electron pairs, then the usable potential length is 65 cm.

The conversion probabilities for  $1\gamma$  and  $2\gamma$  from  $1\pi^0$ ,  $2\gamma$  from  $2\pi^0$ , and  $4\gamma$  from  $2\pi^0$  are given in Table II for different radiation length liquids and different bubble-chamber configurations. The photon conversion length used is  $1.32 X_0$ . By using liquids of shorter radiation length, one gains photon conversion efficiency at the expense of the momentum measurement accuracy. For  $\pi^0$  momentum errors of 10% or less up to about 30 BeV/c, a hydrogen-neon mixture of  $X_0$  between 50 cm and 100 cm is suggested.<sup>10</sup> If a 1.0 m potential length and  $X_0 = 100$  cm (50 cm) is used, then the single  $\gamma$  and  $2\gamma$  from a single  $\pi^0$  and  $4\gamma$ 's from  $2\pi^0$  conversion probabilities are 54% (79%), 29% (62%), and 8.3% (38%) respectively. The probability of a  $2\pi^0$  event converting only two gamma rays is 37% (17%). The advantages of the use of the TST are also obvious from Table II, e. g., the conversion probability for  $4\gamma$  from  $2\pi^0$  is improved by nearly two orders of magnitude by using the TST over a pure hydrogen filling.

#### B. Gas Costs for Various Bubble-Chamber Configurations

To make estimates of the gas filling costs for the 15-ft bubble chamber may be somewhat misleading since the cost of neon is rapidly changing, and the deuterium in principle is owned by the AEC. This notwithstanding, an estimate will be made using the approximate costs of \$100 per  $m^3$  for  $H_2$ , \$43,500 per  $m^3$  for neon, and \$40,000 per  $m^3$  for  $D_2$ . The bubble chamber and TST dimensions are given in Table I. The costs for various chamber and TST fillings are given in Table III.

If a proton target and an analysis region of 50-cm radiation length are desired, then the choice is to use an equal atomic mixture of hydrogen and neon in the chamber with or without a hydrogen-filled TST. By using a TST, the identification of proton events is greatly simplified, and a \$30,000 savings is realized in gas-filling costs. If a neutron target is desired along with an analysis region of 50-cm radiation length, then the TST solution is also the most economical with a net savings of about \$450,000.

Because of the high cost of deuterium, it is most important that a hydrogen-neon blanket be used around the deuterium-filled TST rather than a deuterium-neon blanket. The cost difference between these two blankets for  $X_0 \approx 50$  cm mixtures is on the order of \$0.5 million. This cost differential emphasizes the importance of having separate temperature and pressure controls in the TST w. r. t. the rest of the chamber.

### C. Fraction of Neutrino Flux Passing Through the TST

Relative to the neutrino flux passing through the entire bubble chamber, the fraction of flux,  $F_{TST}$ , which passes through the TST, is dependent on the radius,  $R$ , of the TST and the neutrino energy for a fixed neutrino-beam configuration and a fixed proton bombardment energy. The fiducial region of the bubble chamber projected on the plane normal to the neutrino-beam axis is taken as a disc 1.40 m in radius. For an optimized 200-GeV beam (decay distance = 600 m, shield thickness = 150 m) using the Hagedorn-Ranft model and real focusing,  $F_{TST}$  at different neutrino energies passing through TST's of different radii are given in Fig. 2.

If the flux density across the bubble chamber were constant, then  $F_{TST}$  would vary as shown in Fig. 2 from 4.6% ( $R = 0.3$  m) to 52% ( $R = 1.0$  m). For this beam configuration, neutrinos below about 9 GeV are most concentrated near the outside of the chamber giving  $F_{TST}$  values lower than those for a uniform flux density. At about 9 GeV the neutrino density is about uniform across the chamber. Higher energy neutrinos become concentrated near the center of the chamber. As we increase in neutrino energy, we pass from the pion neutrinos to the kaon neutrinos which, because of the larger center-of-mass energy, are more uniformly distributed across the chamber. In general, for a fixed  $R$ , the  $F_{TST}$  values lie around the uniform density values with the lower energy neutrino values being lower and the higher energy neutrino values being higher.

The neutrino-flux density across the chamber becomes more uniform as the proton energy decreases and as the target-to-detector distance increases. Figure 3 presents the situation for a real-focused 500-GeV beam (decay length = 600 m, shield thickness = 1000 m). It is apparent that in this beam the flux density is more nearly constant over the full neutrino-energy region within  $R = 1.35$  m. For the higher energy neutrino beam, the bubble-chamber fiducial volume radius was taken as 1.35 m.

For a TST of radius 0.74 m, the  $F_{\text{TST}}$  values vary from 15% ( $E_\nu = 5$  GeV) to 56% ( $E_\nu = 30$  GeV) for the 200-GeV beam and from 22% ( $E_\nu = 10$  GeV) to 38% ( $E_\nu = 30$  GeV) for the 500-GeV beam. A uniform-flux density given  $F_{\text{TST}} \approx 30\%$  for both beams. The total neutrino flux averaged over all neutrino energies in the 500-GeV beam has approximately the same  $F_{\text{TST}}$  variation as the 200-GeV neutrino flux.

#### D. The Ratio of Events Inside and Outside the TST

For the two beam conditions used in Section C, the neutrino-flux densities averaged over all neutrino energies were essentially constant over the bubble chamber. Therefore, only the uniform flux density case will be used in this section. More detailed calculations can be made by using the detailed  $F_{\text{TST}}(E_\nu)$  information of the previous section.

The bubble-chamber fiducial volume is defined as that volume common to a 3.8-m diameter sphere and a 2.8-m diameter cylinder all centered on the neutrino-beam axis. The fiducial volume is about  $20 \text{ m}^3$ . The TST volume is determined from the requirements that it be a right circular cylinder terminated by a hemispherical cap and that the potential length in the forward direction outside the TST be 1.0 m. If  $R$  is the TST radius, then the TST volume is approximately  $V_{\text{TST}} = \pi R^2 (2.8 - 0.34 R)$ , and the remaining bubble-chamber volume is  $V_{\text{BC}} = 20 \text{ m}^3 - V_{\text{TST}}$ .

Consider the bubble chamber fitted with a TST of radius  $R$  and of the above specified volume. Assume that the bubble chamber is illuminated on one side with a uniform neutrino-flux density, and the neutrino-proton and neutrino-neutron cross sections are equal, the bubble chamber and TST are operated at  $28^\circ \text{K}$ , then the ratio of neutrino events outside the TST to events inside the TST are presented in Fig. 4 for different TST radii and different fillings. The mixed fillings are expressed as volume fractions.

Curve 7 of Fig. 4 serves as a reference since it represents for a simple hydrogen chamber the inverse fraction of events within a volume of radius  $R$  (and of the TST length). The number of background events, those outside the TST, increases as the TST radius decreases and as the ratio of nucleon densities of the region outside the TST to the region inside the TST increase.

The total neutrino flux passing through a 0.6 m radius TST is  $0.00382/\text{m}^2$  interacting proton for the 500-GeV beam (shield = 1000 m decay = 600 m). Using  $3 \times 10^{13}$  interacting protons per pulse, a pure hydrogen target, and a total average cross section of  $8 \times 10^{42} \text{ m}^2/\nu$ -nucleon, the total event rate in the TST is about 0.1-neutrino interactions per pulse. From curve 5 we have then 2 interactions per pulse in the blanket composed of 15% (volume) Ne + 85% (volume) H. For curve 2 with the blanket composed of 50% (volume) Ne + 50% (volume) H, the event rate in the blanket is 5 per pulse. An acceptable ratio of background events to TST events can be achieved

by choosing either a high beam intensity and a lower concentration of neon in the blanket or a higher neon concentration in the blanket and a lower beam intensity. A not unreasonable compromise between event rate, background rate, cost, and gamma-conversion efficiency is to choose a modest proton intensity (about  $1.5 \times 10^{13}$  interacting proton per pulse) and a blanket mixture of about 50% Ne and 50% H ( $X_0 = 50$  cm, filling cost = \$173,000) which gives for a hydrogen-filled TST one event in 20 pulses.

#### E. Setting Errors in the Bubble Chamber

The subject of the magnitude of the setting error in large bubble chambers has been extensively discussed, and the general feeling is that the setting error lies between  $100\mu$  and  $500\mu$ . Calculations of the probable error of the momentum of electron tracks in H-Ne mixtures have been made for setting errors of  $100\mu^{10}$  and  $500\mu$ .<sup>8</sup> The only point we wish to make is that both estimates of the setting error may be correct when a TST is used. Using the chamber and TST dimensions from Table I and using the downstream triad of cameras from the layout of Fig. 1, we observe that approximately 40% of the volume (above the TST) is visible by all three cameras, 40% of the volume (inside and below the TST) is not visible except by looking through the TST. The other 20% of the volume is visible by one or two cameras directly. Of course, nearly all parts of the chamber are visible by three cameras if you are willing to look through the TST. Our contention is that the setting error could be about  $130\mu$  when one does not look through the TST. If a track must be viewed through the TST by three cameras, the setting error could be as large as  $400\mu$ . Thermal gradients near the TST and distortion caused by the imperfect TST surface could make the region under the TST considerably worse.

#### F. TST Distortion of Track Images

During this summer study several people were concerned with the distorted field of the 15-ft chamber optics. It should be remembered that the TST will act as a cylindrical lens. The end of the TST is a hemispherical lens. Therefore, converted gamma rays viewed through the TST cannot easily be correlated with interactions in the TST, and components of gamma-ray showers cannot easily be identified.

It is impossible to remove these optical distortions if a cylindrical TST is used; however, the effect of these distortions can be minimized by keeping the region downstream of the TST visible by two cameras directly. This can be achieved by not having the length of the TST extend beyond the plane transverse to the beam which contains the two downstream cameras. This TST is called the short TST in Table II. The short TST increases the potential length for photon conversion and only reduces the TST volume by about 20%.

## REFERENCES

- <sup>1</sup>V. P. Kenney et al., Strong-Interaction Physics in the 25-Ft Bubble Chamber, National Accelerator Laboratory 1969 Summer Study Report SS-17, Vol. II, p. 1.
- <sup>2</sup>V. P. Kenney, Neon-Hydrogen Mixtures and Track-Sensitive Targets for Bubble-Chamber Experiments at NAL, National Accelerator Laboratory 1969 Summer Study Report SS-24, Vol. II, p. 249.
- <sup>3</sup>B. Roe, Considerations on the Use of Neon-Hydrogen Double Chambers, National Accelerator Laboratory 1969 Summer Study Report SS-57, Vol. II, p. 239.
- <sup>4</sup>B. Palmer et al., Reconsiderations of a Spherical 25-Foot Bubble Chamber in the Light of Track-Sensitive Targets, National Accelerator Laboratory 1969 Summer Study Report SS-82, Vol. II, p. 225.
- <sup>5</sup>R. Huson, Track Sensitive Targets in the 25-Foot Bubble Chamber, National Accelerator Laboratory 1969 Summer Study Report SS-99, Vol. II, p. 229.
- <sup>6</sup>B. Roe et al., Neutrino Experiments in the 25-Foot Bubble Chamber, National Accelerator Laboratory 1969 Summer Study Report SS-104, Vol. II, p. 91.
- <sup>7</sup>M. Alston-Garnjost, Strong-Interaction Physics in the 25-Ft Bubble Chamber, National Accelerator Laboratory 1969 Summer Study Report SS-140, Vol. II, p. 5.
- <sup>8</sup>C. T. Murphy, Electron Momentum Errors, Single  $\pi^0$  Physics, and  $2\pi^0$  Physics in Hydrogen-Neon Mixtures in the 25-Foot Bubble Chamber, National Accelerator Laboratory 1969 Summer Study Report SS-155, Vol. II, p. 45.
- <sup>9</sup>G. Horlitz et al., Nucl. Instr. and Methods 68 213 (1969).
- <sup>10</sup>C. E. Kalmus, Lawrence Radiation Laboratory Report UCRL-T6830, Vol. III, 1966, p. 230.

Table I. Assumed Bubble-Chamber and TST Parameters.

<u>Bubble Chamber</u>	
Shape	- Sphere of 3.81-m diameter
Volume	- $29 \text{ m}^3$
Camera layout	- six cameras in two triad as shown in Fig. 1
<u>TST</u>	
Shape	- right circular cylinder (1.48 m diameter ) 2.22-m long) terminated with a hemispherical cap
Volume	- $4.7 \text{ m}^3$
TST wall thickness	- 2.54 cm
TST wall volume	- $0.35 \text{ m}^3$

Table II. Photon Conversion Probabilities (%)  
for Various Bubble-Chamber Configurations.

Number of Photon Converted	$x_0$ (m) <sup>a</sup>	$x_c$ (m)	Average Potential Length (m) <sup>b</sup>		
			2.5	1.0	0.65
1 $\gamma$	0.25	0.33	100	95	86
	0.50	0.65	98	79	63
	1.0	1.30	85	54	39
	9.7	12.7	18	7.6	5.0
2 $\gamma$ from 1 $\pi^0$	0.25	0.33	100	91	74
	0.50	0.65	96	62	40
	1.0	1.30	73	29	15
2 $\gamma$ from 2 $\pi^0$	9.7	12.7	3.2	0.57	0.25
	0.25	0.33	0	0.01	8.6
	0.50	0.65	0.2	17	32
	1.0	1.30	9.3	37	34
4 $\gamma$ from 2 $\pi^0$	9.7	12.7	13	2.9	1.3
	0.25	0.33	100	82	41
	0.50	0.65	92	38	16
4 $\gamma$ from 2 $\pi^0$	1.0	1.30	53	8.3	2.4
	9.7	12.7	0.1	0	0

<sup>a</sup> Radiation Lengths Used		<sup>b</sup> Potential Lengths	Configuration
$x_0$ (m)	Liquid	2.5 m	No TST
0.25	Pure Ne	1.0 m	Short TST
0.50	50% Ne + 50% H	0.65 m	Normal TST
1.0	15% Ne + 85% H		
9.7	Pure H		

Table III. Gas Costs for Filling the 15-Ft Bubble Chamber and TST.

Gas Filling		Costs (in \$1,000 units)				
Bubble Chamber (30 m <sup>3</sup> -TST volume)		TST (4.7 m <sup>3</sup> )	H	Ne	D	Total
No TST	100% H	None	3			3
	50% Ne + 50% H <sup>a</sup>	None	1.5	202		203
	50% Ne + 50% D	None		202	600	802
	100% Ne	None		404		404
Ne-H Blanket	50% Ne + 50% H	100% H	2	171		173
	50% Ne + 50% D	100% D	1.5	171	188	360
	15% Ne + 85% H	100% D	2.2	51.2	188	241
Ne-D Blanket	50% Ne + 50% D	100% H	0.5	171	506	677
	50% Ne + 50% D	100% D		171	694	865

<sup>a</sup>Mixtures are expressed as volume fractions.

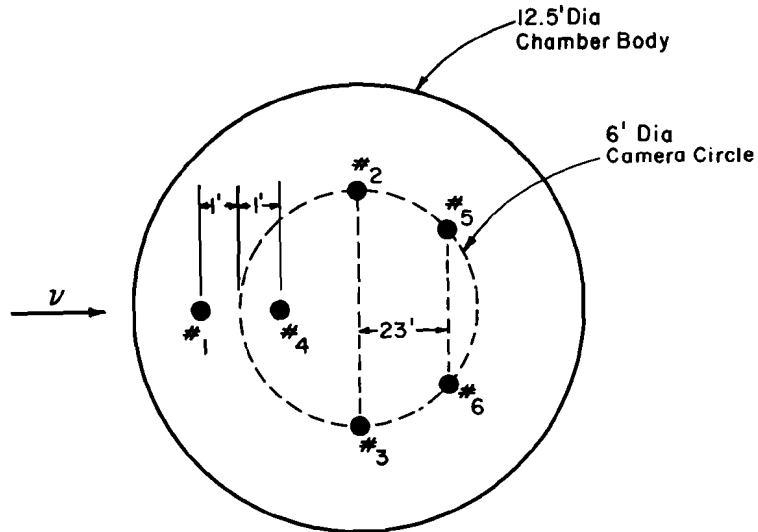


Fig. 1. Camera layout of the 15-ft bubble chamber. Upstream camera triad #1, #2, and #3; downstream camera triad #4, #5, and #6.



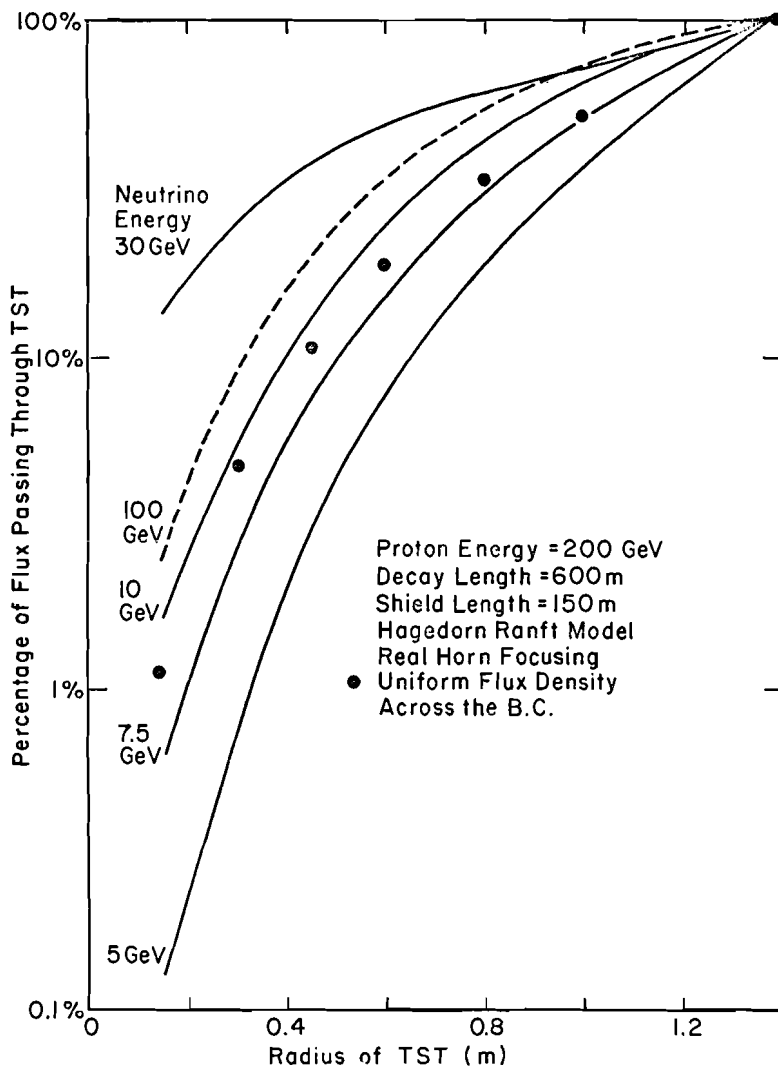


Fig. 2. Fraction of neutrino flux at a given energy passing through TST's of different radii--200 GeV.

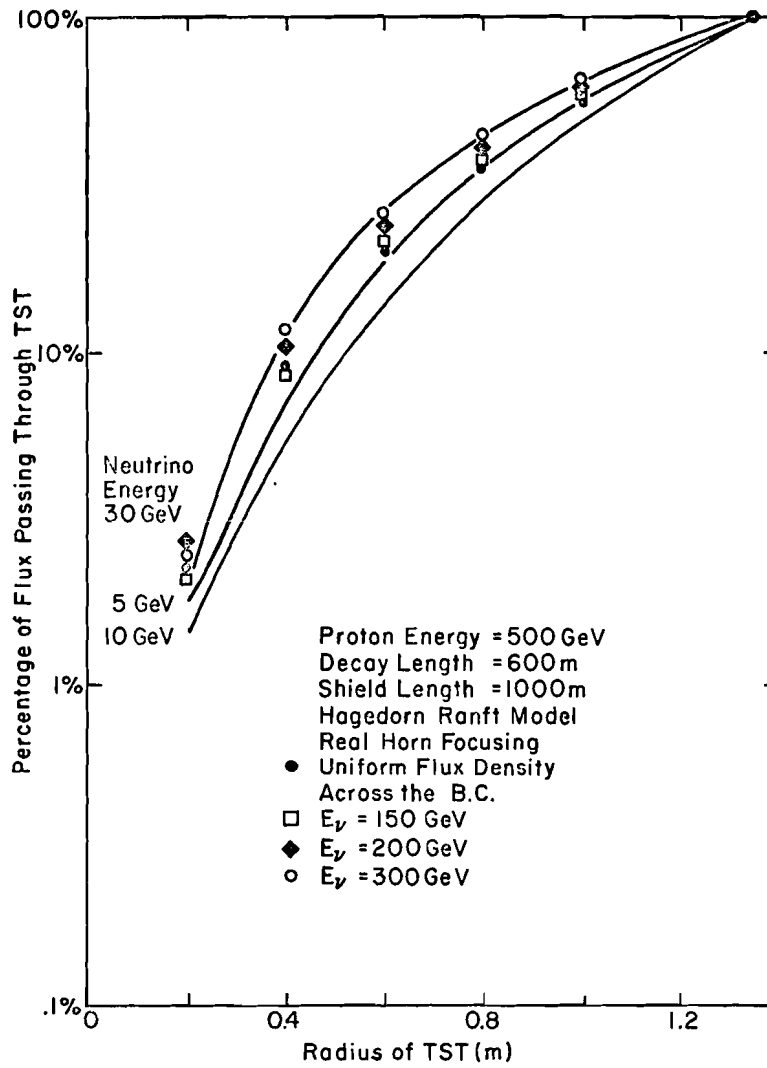


Fig. 3. Fraction of neutrino flux at a given energy passing through TST of different radii--500 GeV.

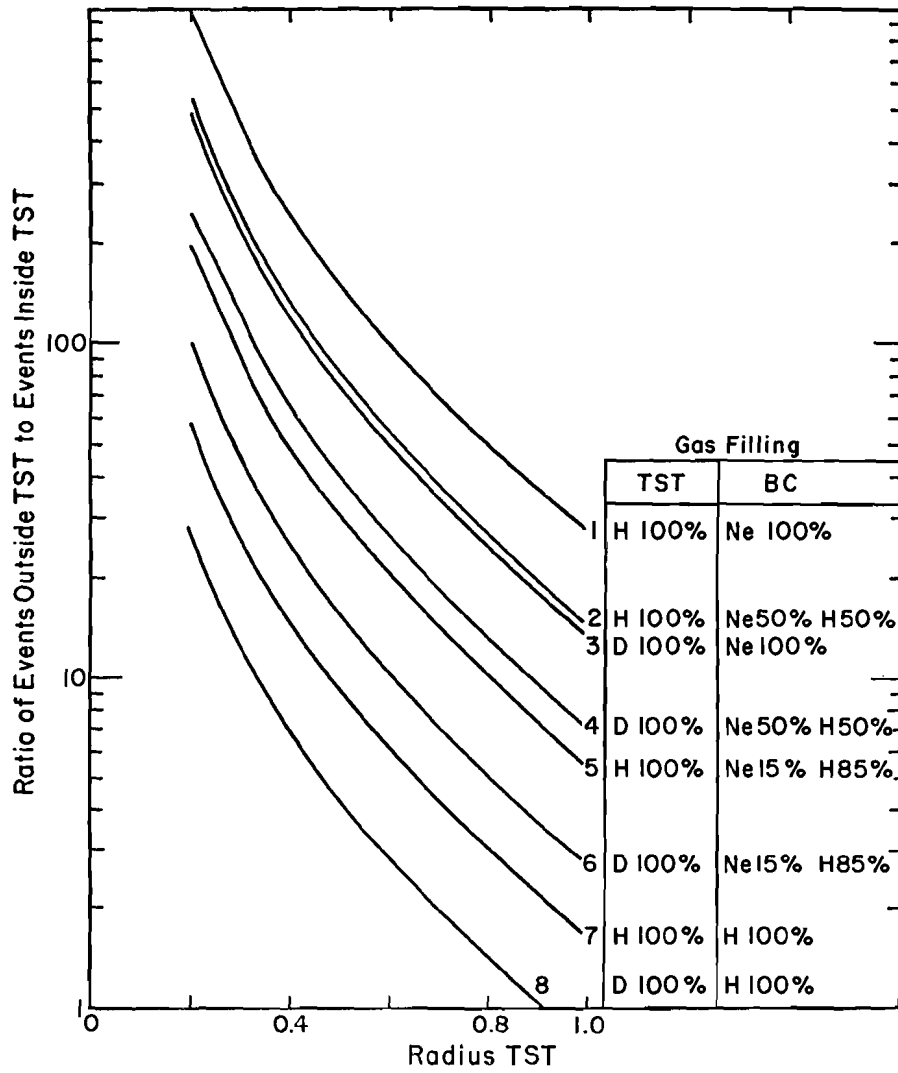


Fig. 4. Ratio of events outside TST to events inside the TST for different TST radii and different fillings.

